Interaction of Environmentally Important Metal Ions with Nitrogen–Sulfur-donor Macrocycles. The Crystal Structures of Seven-co-ordinate Lead(II) and Mercury(II) Complexes of an 18-Membered N_4S_2 Macrocycle†

Alan Bashall, Mary McPartlin, Brian P. Murphy,*‡ Harry R. Powell and Smruti Waikar
School of Chemistry, University of North London, Holloway Road, London N7 8DB, UK

Metal-ion-templated cyclocondensations of two acyclic diamines containing nitrogen and sulfur heteroatoms with pyridine-2,6-dicarbaldehyde in the presence of the ions Pb^{II}, Hg^{II}, Cd^{II} and Ag^{I} afforded 1 : 1 complexes of the appropriate metal ion with the corresponding 18-membered, potentially sexidentate (N_4S_2), diimine macrocycle L^1 or L^2. The soluble lead, mercury and cadmium complexes show strong metal–imine interactions in the NMR spectra: they are rare examples of co-ordination compounds of these ions that exhibit satellites due to proton and carbon-13 coupling to the naturally abundant metal nuclei with spin $I = \frac{1}{2}$. The crystal structures of the complexes $[PbL^1(MeOH)(H_2O)][ClO_4]_2$ **1a** and $[HgL^1(SCN)_2]\cdot MeOH$ **2** have been determined. In both complexes the macrocycle adopts a stepped conformation with respect to the two pyridyl units; this conformation facilitates *endo*-dentate configurations for the sulfur donors which interact through long bonds to the metal which, in turn, is located towards the trimethine part of the macrocycle. The combination of the asymmetrical location of the metal ion within the macrocyclic cavity and the long bonds to the sulfurs leaves the second pyridine nitrogen remote and unco-ordinated. The metal geometry in **1a** is best described as a very distorted *nido*-hexagonal bipyramid in which the macrocycle donors occupy five of the six 'equatorial' sites and solvent molecules define severely bent 'axial' positions, implicating a stereochemically active role for the $6s^2$ lone-pair electrons on Pb^{II}. The structure of **2** is similar to that of **1a** but the axial positions are linear and occupied by thiocyanate ions; in contrast to **1a**, the mercury atom is displaced well out of the plane of the trimethine co-ordinating fragment. Both are rare examples of structural characterisations of the interaction of mixed nitrogen–sulfur-donor macrocycles with these toxic heavy-metal ions.

The co-ordination chemistry of the toxic and precious heavy-metal ions is of crucial importance to the design of complexing agents which may serve as sensors or extractants of these metals for biological, environmental or recycling purposes. The development of technologies to these ends will rely, at source, on the ability of a compound selectively or specifically to bind metal-ion types or individual metal ions respectively. With regard to metal-ion selectivity, macrocycles have been widely studied, some of their efficacy in this respect being attributed to 'best-fit' and structural dislocation phenomena.[1]

Further to our previous interests in the co-ordination chemistry of such ions,[2] we report here the synthesis of two 18-membered, mixed-donor, nitrogen–sulfur macrocycles, L^1 and L^2, and their interaction with the metal ions Pb^{II}, Hg^{II}, Cd^{II} and Ag^{I}. Despite the fact that during the course of this work Constable *et al.*[3] published the synthesis of $[PbL^2(NCS)_2]$, we include our brief description of this compound as prepared by alternative means together with additional findings; our work has been presented in a preliminary form.[4] The crystal structures of $[PbL^1(MeOH)(H_2O)][ClO_4]_2$ **1a** and $[HgL^1(SCN)_2]\cdot MeOH$ **2** are also reported herein.

The 18-membered mixed-donor macrocycles L^1 and L^2 were designed with regard to the borderline hard/soft characteristics of these environmentally important metals. Further, previous studies on macrocyclic ligands have demonstrated that 18-membered, sexidentate rings are well suited to the incorporation of metal ions of this type.[3,5–7]

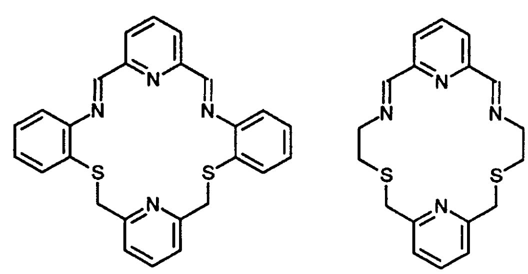

L^1 L^2

† *Supplementary data available:* see Instructions for Authors, *J. Chem. Soc., Dalton Trans.*, 1994, Issue 1, pp. xxiii–xxviii.

‡ *Present address:* Department of Chemistry, John Dalton Building, Manchester Metropolitan University, Chester Street, Manchester M1 5GD.

Experimental

Instrumentation.—Infrared spectra were recorded using either a Perkin Elmer 781 or a Biorad FTS40 spectrophotometer. A Carlo Erba 1106 elemental analyser was used for microanalytical determinations. Mass spectra were recorded on a Kratos Profile GC-MS instrument: fast atom bombardment (FAB) mass spectra were obtained from the SERC mass spectrometry service at University College, Swansea. Proton and carbon-13 NMR spectra were obtained using a Bruker AM-250 spectrometer.

Syntheses.—Unless otherwise stated, all materials used were obtained commercially. 2,6-Bis(bromomethyl)pyridine[8] and pyridine-2,6-dicarbaldehyde[9] were both prepared

Table 1 Elemental microanalytical,[a] selected mass spectral[b] and selected infrared[c] data for the complexes of L^1 and L^2

	Analysis (%)			Mass spectrum			Infrared spectrum (cm^{-1})		
Complex	C	H	N	m/z	(%)	Assignment	ν(C=N)	Anion	Colour
$[PbL^1][ClO_4]_2$	36.3 (36.4)	2.4 (2.4)	6.5 (6.5)	759 658	(100) (55)	$[PbL^1(ClO_4)]^+$ $[PbL^1]^+$	1622	1060, 624	Orange
$[PbL^1][NO_3]_2$	39.9 (39.8)	2.8 (2.6)	10.6 (10.7)	722 660	(55) (21)	$[PbL^1(NO_3)]^+$ $[PbL^1]^+$	1630	1390, 822	Orange
$[PbL^1(NCS)_2]$	43.3 (43.3)	2.5 (2.6)	10.8 (10.6)	718 660	(100) (35)	$[PbL^1(NCS)]^+$ $[PbL^1]^+$	1620	2040	Orange
$[PbL^1]Cl_2$	42.8 (42.7)	2.7 (2.8)	7.7 (7.7)				1620		Orange
$[HgL^1(SCN)_2]\cdot MeOH$	43.3 (43.7)	3.0 (2.6)	10.8 (10.9)	712 453	(100) (35)	$[HgL^1(SCN)]^+$ $[L^1]^+$	1622	2120	Yellow
$[CdL^1][ClO_4]_2$	40.7 (40.9)	2.8 (2.6)	7.4 (7.3)	565 355	(5) (100)	$[CdL^1]^+$ $[L^1H]^+$	1630	1090, 620	Yellow
$[CdL^1][NO_3]_2\cdot MeCN$	46.7 (46.1)	3.2 (4.0)	13.7 (13.4)	628 565	(100) (90)	$[CdL^1(NO_3)]^+$ $[CdL^1]^+$	1630	1390	Yellow
$[CdL^1(NCS)_2]$	49.9 (49.4)	2.9 (3.0)	12.5 (12.3)	624 565	(96) (56)	$[CdL^1(NCS)]^+$ $[CdL^1]^+$	1620	2070	Yellow
$[AgL^1]ClO_4$	45.9 (46.1)	2.9 (3.3)	8.6 (8.3)	561	(100)	$[AgL^1]^+$	1630	1100, 630	Orange
$[AgL^1]NO_3$	50.5 (50.2)	2.6 (3.2)	11.6 (11.3)	561	(100)	$[AgL^1]^+$	1630	1390	Yellow
$[AgL^1(NCS)]\cdot 2H_2O$	51.0 (50.9)	4.0 (3.6)	11.5 (10.9)				1630	2090	Orange
$[PbL^2(NCS)_2]$[d]	32.5 (31.8)	3.0 (3.0)	12.5 (12.4)	622 564	(75) (14)	$[PbL^2(NCS)]^+$ $[PbL^2]^+$	1650	2080	Yellow
$[PbL^2Br_2]$	30.4 (29.9)	2.8 (2.8)	7.7 (7.8)	643 564	(89) (11)	$[PbL^2(Br)]^+$ $[PbL^2]^+$	1660		Yellow

[a] Required values in parentheses. [b] Fast atom bombardment, 3-nitrobenzyl alcohol matrix, positive-ion mode. [c] As KBr discs. [d] Reported previously by an alternative route.[3]

from 2,6-bis(hydroxymethyl)pyridine according to literature methods.

2,6-Bis(2-aminothiophenoxymethyl)pyridine. To a stirring solution of sodium ethoxide (2.4 g sodium in 150 cm^3 ethanol) and 2-aminothiophenol (12.8 g, 0.1 mol) in ethanol (100 cm^3) at room temperature and under an atmosphere of nitrogen, was added, dropwise over a period of 30 min, a solution of 2,6-bis(bromomethyl)pyridine (13.6 g, 0.05 mol) in ethanol (100 cm^3). The solution was refluxed for 4 h, cooled to room temperature, and poured into an equal volume of water. Upon standing, white flocculent crystals were obtained which were filtered off, washed with water and dried over P_2O_5 (Found: C, 64.6; H, 5.4; N, 11.8. Calc. for $C_{18}H_{18}N_3S_2$: S, 64.6; H, 5.4; N, 11.9%). Mass spectrum (electron impact, EI): m/z 353. Infrared (KBr disc): ν(NH) 3440, 3340; δ(NH_2) 1620; ν(C=C) and ν(C=N) 1590(sh) cm^{-1}. NMR (CD_3CN, relative to $SiMe_4$, 298 K): ^1H (250.133 MHz), δ 7.42 (t, 1 H, py), 7.15 (dd, 2 H, C_6H_4), 7.05 (ddd, 2 H, C_6H_4), 6.92 (d, 2 H, py), 6.69 (dd, 2 H, C_6H_4), 6.50 (td, 2 H, C_6H_4), 4.70 (s, 4 H, NH_2) and 3.94 (s, 4 H, CH_2); ^{13}C (62.896 MHz), δ 158.75, 150.40, 137.75, 136.96, 130.94, 122.32, 118.29, 117.10, 115.54 and 41.38.

$[PbL^1]X_2$ (X = ClO_4^-, NO_3^-, NCS^- *or* Cl^-). The appropriate lead(II) salt (0.6 mmol) was dissolved, or suspended, together with pyridine-2,6-dicarbaldehyde (0.08 g, 0.6 mmol) in methanol (50 cm^3). To the aforementioned stirred solution, 2,6-bis(2-aminothiophenoxymethyl)pyridine (0.2 g, 0.6 mol) was added dropwise as a solution in methanol (50 cm^3) to produce an immediate colour change from colourless to bright orange. After a 1 h reflux, the solution was allowed to stand for 24 h to give the appropriate complexes as orange solids. The complexes were filtered off, washed with ice-cold methanol and air-dried. For the X-ray crystallographic study the complex $[PbL^1][ClO_4]_2$ **1** was further recrystallised from methanol–water to give $[PbL^1(MeOH)(H_2O)][ClO_4]_2$ **1a**.

$[AgL^1]X$ (X = ClO_4^-, NO_3^- *or* NCS^-). The perchlorate or nitrate salt of silver(I) (0.6 mmol) and pyridine-2,6-dicarbaldehyde (0.08 g, 0.6 mmol) were dissolved together in methanol (50 cm^3). 2,6-Bis(2-aminothiophenoxymethyl)pyridine (0.2 g, 0.6 mol) was added dropwise, with stirring, as a solution in methanol (50 cm^3). After a 1 h reflux period the resultant dark orange solid was filtered off and recrystallised twice from acetonitrile to give yellow solids which were recovered by filtration, washed with methanol followed by diethyl ether and dried *in vacuo*. The thiocyanate derivative was obtained from the perchlorate by anion metathesis in methanol using LiNCS.

$[HgL^1(SCN)_2]\cdot MeOH$ **2**. To a stirring suspension of $Hg(SCN)_2$ (0.18 g, 0.6 mmol) in a solution of pyridine-2,6-dicarbaldehyde was added dropwise 2,6-bis(2-aminothiophenoxymethyl)pyridine (0.2 g, 0.6 mmol) as a solution in methanol (50 cm^3). The resultant bright orange solution was refluxed for 1 h, filtered whilst hot, and the filtrate allowed to stand overnight at 4 °C. Orange crystals of complex **2** were filtered off, washed with cold methanol followed by diethyl ether and dried *in vacuo*.

$[CdL^1]X_2$ (X = ClO_4^-, NO_3^- *or* NCS^-). To a stirred solution of cadmium(II) perchlorate or nitrate (0.6 mmol) and pyridine-2,6-dicarbaldehyde in methanol (50 cm^3) was added dropwise a solution of 2,6-bis(2-aminothiophenoxymethyl)pyridine (0.2 g, 0.6 mmol) in methanol (50 cm^3). The resulting pale yellow solution was refluxed for 1 h and then allowed to stand at 4 °C for several days. The resultant solid was recovered and recrystallised from methanol–acetonitrile (3:1) to give the purified complexes which were filtered off, washed with cold methanol followed by diethyl ether and dried *in vacuo*. The thiocyanate derivative was obtained by anion metathesis of the perchlorate using LiNCS in methanol.

$[PbL^2Br_2]$. (*i*) To a stirring solution of sodium ethoxide (2.4 g sodium in 300 cm^3 ethanol) and 2-aminoethane-1-thiol hydrochloride (9.05 g, 0.08 mol) at room temperature and under an atmosphere of nitrogen was added dropwise over a period of 30 min a solution of 2,6-bis(bromomethyl)pyridine in ethanol (100 cm^3). After a reflux period of 4 h a precipitate of sodium salts was filtered off and the filtrate used in (*ii*) without further purification.

Table 2 Proton and carbon-13 NMR data[a] corresponding to L^1 for the CD_3CN-soluble complexes $[PbL^1][ClO_4]_2$ **1**, $[HgL^1(SCN)_2]\cdot MeOH$ **2**, $[CdL^1][ClO_4]_2$ **3** and $[AgL^1]ClO_4$ **4**

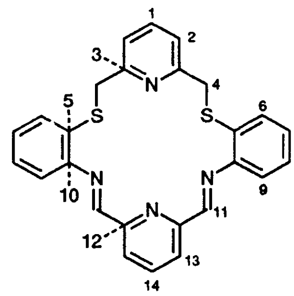

Proton[b]	1	2	3	4
H^{11}	9.57(s)[c]	9.06(s)[c]	9.15(s)[c]	8.86(s)
H^{14}	8.62(t)	8.38(t)	8.58(t)[c]	8.31(t)
H^{13}	8.35(d)	8.13(d)	8.36(d)[c]	8.05(d)
H^6 or H^9	7.91	7.82	7.81(dd)	7.77(dd)
	(m)	(m)		
H^1	7.83	7.75	7.91(t)	7.65(t)
H^7, H^8, H^9 or H^6	7.63	7.53	7.67	7.53
	(m)	(m)	(m)	(m)
	7.48	7.40	7.45	7.36
H^2	7.49(d)	7.40(d)	7.45(d)	7.25(d)
H^4	4.75(s)	4.55(s)	4.36(s)	4.35(s)
Carbon-13[d]				
C^{11}	164.46	158.39	160.64[c]	
C^{12}	157.22	156.64	155.54[c]	
C^3	153.97	151.01	148.30[c]	
C^{10}	149.76	148.18	147.42[c]	
C^{14}	143.54	142.15	145.01[c]	
C^1	140.46	139.59	142.45	
C^{13}	133.60	132.25	133.25[c]	
C^{ar}	133.08	133.59	135.29	
C^5	132.83	133.40	126.47	
C^2	131.20	130.13	126.38	
C^{ar}	130.68	130.05	132.39	
C^{ar}	124.85	124.13	130.75	
C^{ar}	121.94	121.48	122.13	
C^4	42.86	43.75	42.77	

[a] Values in ppm relative to $SiMe_4$ at 25 °C (250.134 MHz for protons and 62.896 MHz for carbons). [b] Integrations are as expected for L^1. [c] Metal satellites corresponding to coupling to ^{207}Pb, ^{199}Hg or $^{113/111}Cd$ observed (see Table 4 for details). [d] $C^{ar} = C^6–C^9$.

Table 3 Proton and carbon-13 NMR data[a] corresponding to L^2 for the complex $[PbL^2(NCS)_2]$.

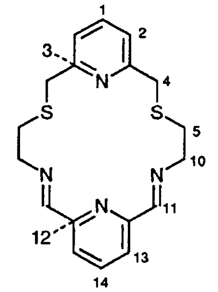

Proton	δ	Carbon[b]	δ
H^{11}	9.60(s)[c]	C^{11}	164.21[c]
		C^{12}	157.52
		C^3	153.40[c]
H^{14}	8.63(t)[c]	C^{14}	142.65[c]
H^{13}	8.38(d)	C^{13}	130.87[c]
H^1	7.90(t)	C^1	139.68
H^2	7.53(d)	C^2	123.67
H^{10}	4.46(m)	C^{10}	58.53
H^4		C^4	37.29
H^5	3.32(m)	C^5	33.75

[a] Values in ppm relative to $SiMe_4$ at 25 °C, 250.134 or 68.896 MHz, solvent $[^2H_7]$dimethylformamide. [b] For ease of comparability with L^1; $C^6–C^9$ inclusive do not exist for L^2. [c] Lead-207 satellites.

Table 4 Summary of metal satellites in the proton NMR spectra of complexes **1–5**

			Intensity[b]	
Complex[a]	Coupling	J/Hz	Found	Required[c]
1	$^3J(H^{11}–^{207}Pb)$	16.7	*d*	
2	$^3J(H^{11}–^{199}Hg)$	7.2	4.9:1	4.9:1
3	$^3J(H^{11}–^{113/111}Cd)$	30.4	2.9:1	3.0:1
3	$^4J(H^{13}–^{113/111}Cd)$	4.1	*d*	
5	$^3J(H^{11}–^{207}Pb)$	15.9	3.6:1	3.4:1

[a] Complexes **1–4** as in Table 2; **5** is $[PbL^2(NCS)_2]$. [b] Measured relative to the central proton signal. [c] As calculated from natural abundances of the $I = \frac{1}{2}$ isotopes. [d] Resolution poor due to overlap with the central proton signal.

(*ii*) The salt $Pb(ClO_4)_2\cdot 3H_2O$ (0.2 g, 0.4 mmol) and pyridine-2,6-dicarbaldehyde (0.06 g, 0.4 mmol) were dissolved in methanol (20 cm^3). To this solution was added dropwise with stirring and heating 20 cm^3 of the filtrate from (*i*). After 15 min a yellow solid began to precipitate. It was filtered off, washed with methanol followed by diethyl ether and dried over P_2O_5.

$[PbL^2(NCS)_2]$. A suspension of $[PbL^2Br_2]$ (0.1 g, 0.14 mmol) was refluxed in dimethylformamide (40 cm^3) in the presence of an excess of LiNCS to give a clear yellow solution. After filtration whilst hot, the solution produced yellow crystals upon standing. They were filtered off, washed with water followed by ethanol then diethyl ether and dried *in vacuo*.

X-Ray Structural Analyses.—Crystal data. $C_{26}H_{26}Cl_2N_4O_{10}PbS_2$ **1a**, M = 908.74, triclinic, space group $P\bar{1}$ (no. 2), a = 13.037(4), b = 11.673(3), c = 10.844(3) Å, α = 93.93(2), β = 101.13(3), γ = 94.82(2)°, Z = 2, U = 1607.41 Å^3, D_c = 1.878 g cm^{-3}, $F(000)$ = 888, μ(Mo-Kα) = 55.9 cm^{-1}.

$C_{29}H_{24}HgN_6OS_4$ **2**, M = 801.39, triclinic, space group $P\bar{1}$ (no. 2), a = 13.65(4), b = 12.085(4), c = 9.393(3) Å, α = 89.64(2), β = 97.17(3), γ = 102.96(3)°, Z = 2, U = 1498.58 Å^3, D_c = 1.878 g cm^{-3}, $F(000)$ = 784, μ(Mo-Kα) = 53.90 cm^{-1}.

Data collection. Data were collected in the range θ 3–25° using a Philips PW1100 diffractometer, with a scan width of 0.90° for both crystals, using the technique described previously.[10] A pale orange crystal of size 0.35 × 0.24 × 0.34 mm for complex **1a** and an orange crystal of size 0.26 × 0.08 × 0.16 mm for **2** were used in the data collection. Three reference reflections were measured every 5 h in each case and showed no significant changes in intensities. The data were corrected for Lorentz and polarisation factors and equivalent reflections were merged to give a total of 3713 (**1a**) and 2839 (**2**) unique data with $I > 3\sigma(I)$.

Structure solution and refinement.[11] For each structure the coordinates of the metal atom were deduced from a Patterson synthesis. The remaining non-hydrogen atoms were located from subsequent Fourier-difference syntheses. After several cycles of refinement with isotropic thermal parameters, the hydrogen atoms were included at calculated positions (C–H 1.08 Å) with fixed isotropic thermal parameters of 0.08 Å^2. Empirical absorption corrections (**1a**, I_{min} = 0.983, I_{max} = 1.018; **2**, I_{min} = 0.837, I_{max} = 1.196) were applied to both structures at this stage.[12] In the final cycles of full-matrix refinement all the non-hydrogen atoms were assigned anisotropic thermal parameters. Neutral scattering factors, corrected

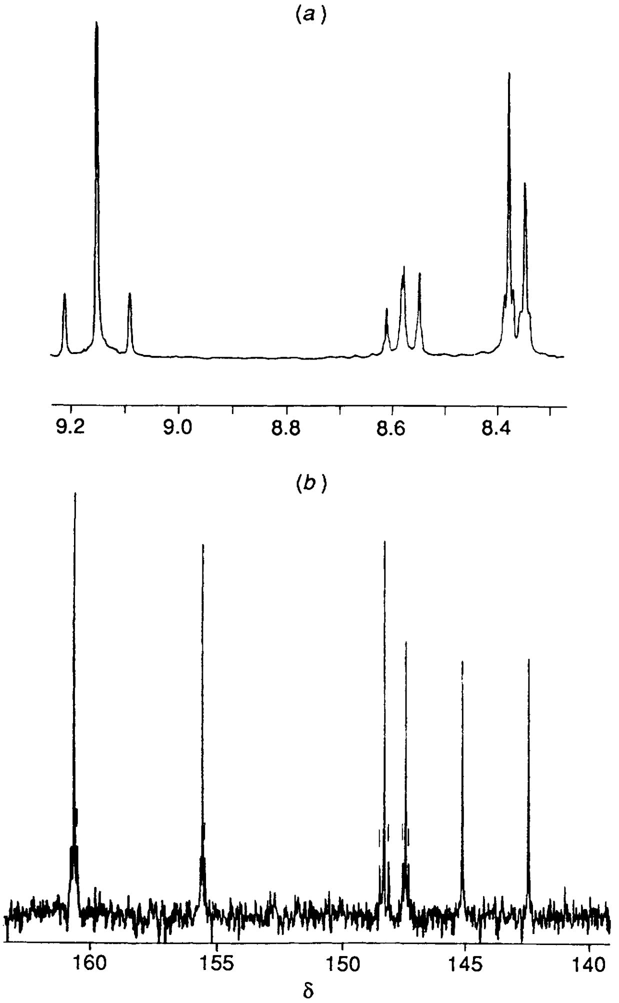

Fig. 1 Partial NMR spectra of $[CdL^1][ClO_4]_2$ showing $^{113/111}Cd$ satellites (ppm scale): (*a*) proton; (*b*) carbon-13

for the real and imaginary components of anomalous dispersion, were used throughout.[13]

Individual weights of $I/[\sigma(F_o)]$ were assigned to each reflection and refinement converged at R 0.0500 and R' 0.0470 for complex **1a** and R 0.0449 and R' 0.0414 for **2**, where $R' = \Sigma||F_o| - |F_c||w^{\frac{1}{2}}/\Sigma|F_o|w^{\frac{1}{2}}$. Atomic coordinates of **1a** and **2** are listed in Tables 7 and 8, selected bond lengths and interbond angles in Tables 5 and 6.

Additional material available from the Cambridge Crystallographic Data Centre comprises H-atom coordinates, thermal parameters and remaining bond lengths and angles.

Results and Discussion

Physical data for the macrocyclic ligands and complexes are summarised in Tables 1 (microanalysis, mass and IR spectral data), 2 and 3 (proton and carbon-13 NMR spectra of complexes of L^1 and L^2 respectively), and Table 4 (metal–proton coupling in NMR spectra). All the complexes were prepared according to well established template procedures[5] in which the Schiff-base macrocyclic ligand has been condensed from the appropriate diamine and pyridine-2,6-dicarbaldehyde in the presence of a heavy-metal ion Pb^{II}, Hg^{II}, Cd^{II} or Ag^{I}. The precursor amine to L^1, 2,6-bis(2-aminothiophenoxymethyl)pyridine, was isolated and characterised (physical data are summarised in the Experimental section); however, in the case of L^2, and in contrast to the method of Constable *et al.*[3] and of Teixidor *et al.*,[14] it was not isolated but generated *in situ*. Attempts to template the macrocyclisations using the Group II metal ions Ca^{II}, Sr^{II} and Ba^{II} did not yield characterisable products, nor did non-template synthesis in the absence of a metal ion.

Infrared data confirm the presence of imine (*ca.* 1620–1660 cm^{-1}) and the absence of carbonyl and amine functional groups of the starting materials. The imine range for the complexes of L^1 (1620–1630 cm^{-1}) is lower than for L^2 (1650–1660 cm^{-1}) but is consistent with a degree of extended delocalisation in L^1 involving the phenylene parts of the macrocycle. Nitrate and perchlorate anion stretches were often obscured by ligand stretches, were broadened and, in some cases, split due to either co-ordination or hydrogen bonding, making assignments of co-ordination modes unreliable. In the case of the thiocyanate anion the high value of 2120 cm^{-1} obtained for the mercury complex $[HgL^1(SCN)_2]$ is indicative of terminal sulfur co-ordination, while the lower values obtained for the corresponding lead and cadmium complexes of L^1 and L^2 are assigned to terminal nitrogen co-ordination. In the case of $[PbL^2(NCS)_2]$ it is clear from comparison of the infrared data in this work and that of Constable *et al.*[3] that the different method of synthesis used has resulted in the isolation of a thiocyanate co-ordination isomer: we find only a single sharp absorption at 2080 cm^{-1}.

Further evidence for the formation of 1 : 1 metal–macrocycle complexes was confirmed in each case by elemental analyses and, in most cases by fast atom bombardment mass spectrometry (Table 1). Parent-ion peaks in the mass spectra are as expected for the mononuclear complexes of a 1 + 1 diimine-containing macrocyclic product. Peaks corresponding to the sequential loss of counter ions are also common.

The orange and yellow colours of the complexes (Table 1) are attributed to metal-perturbed charge-transfer transitions within the imine functionalities of the macrocycles. Neither the precursor amines nor the aldehyde are coloured and, further, the corresponding complexes of the reduced (secondary amine) derivatives of macrocycles L^1 and L^2 are also colourless.[4]

The proton and carbon-13 NMR spectra for the soluble complexes (Tables 2–4) are consistent with the proposed formulations; Table 3 includes data not previously reported for the compound $[PbL^2(NCS)_2]$. Assignments were achieved with the aid of heteronuclear correlation spectroscopy (^1H–^{13}C COSY), distortionless enhancements by polarisation transfer (DEPT 45) spectroscopy, and substituent shift calculations. The most striking feature of the NMR spectra is, with the exception of Ag^I, the rare observation of satellites attributable to proton or carbon coupling to the naturally abundant $I = \frac{1}{2}$ nuclei of the metals, reflecting kinetic inertness in the complexes as well as a degree of covalency in the interaction with a nearby donor atom. The exceptional result for $[AgL^1]ClO_4$ is ascribed to fast exchange of the metal in solution, this proposition being reasonable in view of the propensity of the metal for low co-ordination numbers. The satellite phenomenon is best illustrated by the complex $[CdL^1][ClO_4]_2$, partial spectra of which are reproduced in Fig. 1. Where the satellites are sufficiently well resolved to allow reliable measurements, the intensities relative to the central peak correspond, within experimental error, to the relative natural abundances of the appropriate nuclei (Table 4). It is noteworthy that the three-bond coupling constant, $^3J(H^{11}\text{–}^{113/111}Cd) = 30$ Hz, measured in this work, is of a similar magnitude to a comparable constant of 22 Hz obtained from cadmium-113 NMR studies of the closely related complex $[CdL^3][ClO_4]_2$ where L^3 corresponds to the 18-membered, N_6, tetraimine analogue of L^1.[15] The extent of the observation of satellites in each case gives an indication of the strength of the interaction between the metal and the N_3 and NS_2 donor moieties of the macrocycle. Thus Cd^{II}, Hg^{II} and Pb^{II} all show a strong interaction with the trimethine N_3 donor group, while in the case of Cd^{II} only is there a detectable interaction also with the second pyridyl ring of the ligand.

In summary, the macrocycles reported have only been obtained as complexes of the template-effective ions Pb^{II}, Hg^{II},

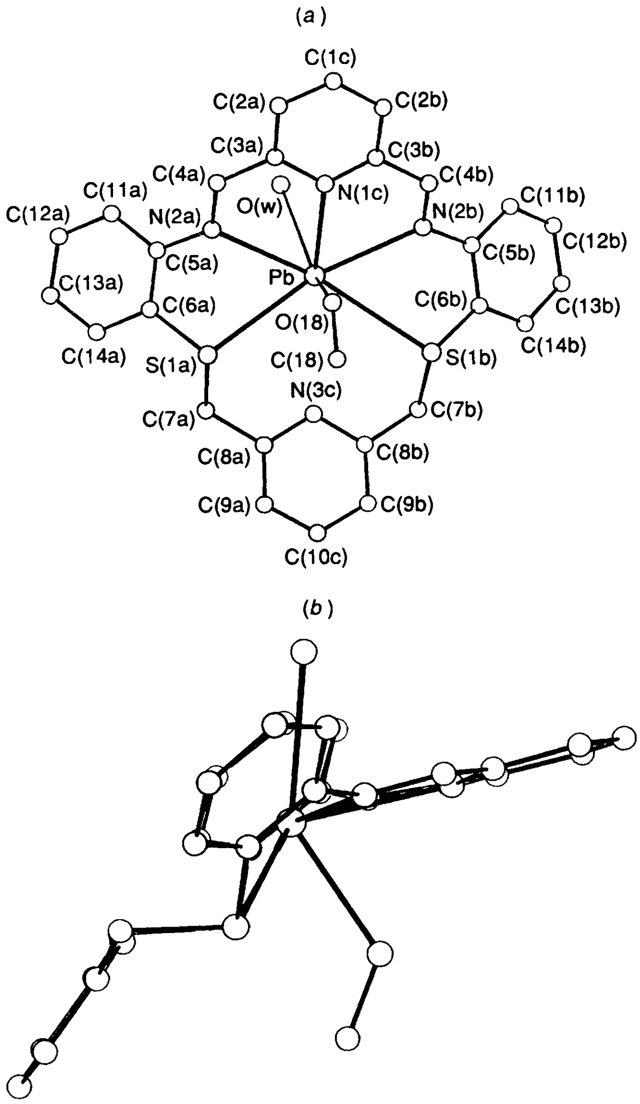

Fig. 2 Structure of $[PbL^1(MeOH)(H_2O)][ClO_4]_2$: (*a*) view showing atom labelling and metal–donor interactions; (*b*) view showing macrocycle conformation and possible location of a stereochemically active lone pair on the lead

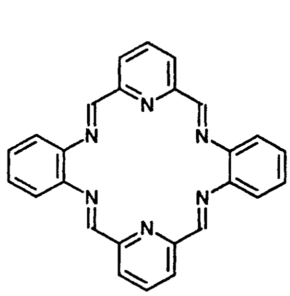

L³

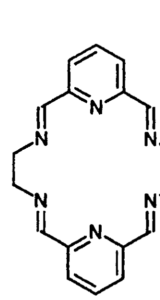

L⁴

Cd^{II} or Ag^{I}. The physical data demonstrate a 1:1 metal:ligand stoichiometry with a dominant interaction between the metal and the trimethine part of the macrocycle. The closely related N_6 macrocycles, L^3 and L^4, do not exhibit the same degree of selectivity in template: in contrast, these ligands are templated on the ions Ca^{II}, Sr^{II}, Ba^{II} and Pb^{II}.[7] Clearly, the substitution of sp^3-hybridised sulfur donors for sp^2-hybridised nitrogens has introduced steric and electronic factors in the template process which give rise to metal-ion discrimination effects. In view of the above, X-ray crystallographic studies were of interest in elucidating the nature of the metal–sulfur interaction in the complexes.

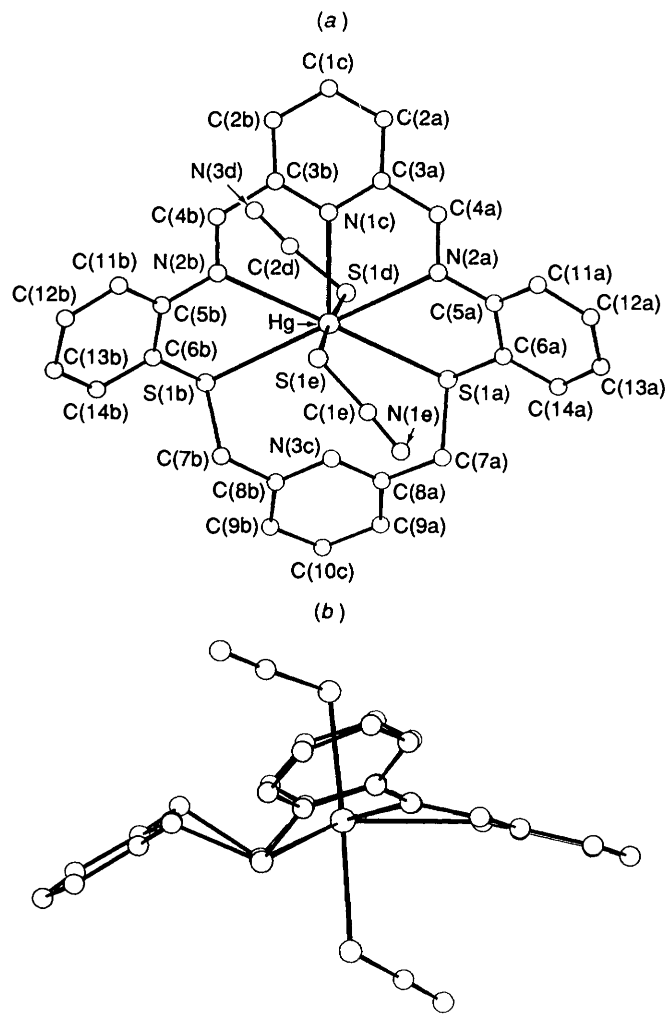

Fig. 3 Structure of $[HgL^1(SCN)_2)]\cdot MeOH$: (*a*) view showing atom labelling and metal–donor interactions; (*b*) view showing macrocycle conformation and disposition of the mercury atom

The crystal structure of the cation of complex **1a** is illustrated in Fig. 2, and selected bond lengths and angles in Table 5. The geometry at the lead atom is best described as very distorted *nido*-hexagonal bipyramidal with L^1 occupying five of the six 'equatorial' sites and one pyridine nitrogen remaining unco-ordinated; one water molecule and one methanol molecule define bent 'axial' co-ordination sites. The lead atom is displaced asymmetrically within the macrocyclic cavity, co-planar with the N_3 trimethine end of the ligand, and 0.69 Å out of the mean plane defined by the five equatorial donor atoms towards the co-ordinated H_2O. The Pb–N bond distances [2.692(9), 2.697(11) and 2.565(9) Å] are typical for the interaction of lead with imine and pyridine nitrogens in related systems.[3] The intramolecular separation between the metal and the pyridine nitrogen, Pb $\cdots$ N(3c), at 3.26 Å is longer than the 2.92 Å found in the crystal structure of $[PbL^2(O_2CMe)(PF_6)]PF_6$;[3] moreover, the tilt of the pyridyl ring is not consistent with a strong interaction with the lead. The Pb–S interactions at 3.146(3) and 3.192(3) Å are long in comparison to the Pb–N but are in the same range as found previously in the structure of $[PbL^2(O_2CMe)(PF_6)]PF_6$;[3] they are also comparable with the other rarely reported lead–thioether distances in the literature.[16] The non-co-ordination of the second pyridyl nitrogen is, at least in part, a consequence of these long Pb–S interactions. While ions such as Pb^{II} and Hg^{II} are not truly ionic, the model of Shannon[17] provides useful data for qualitative,

Table 5 Selected bond lengths (Å) and angles (°) for complex **1a**

Pb–S(1a)	3.146(3)	Pb–S(1b)	3.192(3)	N(2a)–C(5a)	1.401(14)	N(2b)–C(4b)	1.282(13)
Pb–N(1c)	2.565(9)	Pb–N(2a)	2.692(9)	N(2b)–C(5b)	1.417(13)	N(3c)–C(8a)	1.349(14)
Pb–N(2b)	2.697(9)	Pb–O(18)	2.530(8)	N(3c)–C(8b)	1.353(14)	C(3a)–C(4a)	1.452(16)
Pb–O(w)	2.766(8)	S(1a)–C(6a)	1.769(12)	C(5a)–C(6a)	1.377(16)	C(7a)–C(8a)	1.530(17)
S(1a)–C(7a)	1.809(12)	S(1b)–C(6b)	1.757(12)	C(3b)–C(4b)	1.480(15)	C(5b)–C(6b)	1.422(15)
S(1b)–C(7b)	1.816(12)	N(1c)–C(3a)	1.364(14)	C(5b)–C(11b)	1.403(15)	C(6b)–C(14b)	1.399(15)
N(1c)–C(3b)	1.319(14)	N(2a)–C(4a)	1.283(14)	C(7b)–C(8b)	1.500(15)		
N(3c) ··· Pb	3.26	O(11) ··· Pb	3.16	O(13) ··· Pb	3.02		
S(1b)–Pb–S(1a)	107.0(1)	N(1c)–Pb–S(1a)	113.3(2)	C(7b)–S(1b)–C(6b)	102.3(5)	C(3a)–N(1c)–Pb	119.6(7)
N(1c)–Pb–S(1b)	112.0(2)	N(2a)–Pb–S(1a)	59.2(2)	C(3b)–N(1c)–Pb	123.3(7)	C(3b)–N(1c)–C(3a)	116.9(9)
N(2a)–Pb–S(1b)	156.7(2)	N(2a)–Pb–N(1c)	63.9(3)	C(4a)–N(2a)–Pb	115.9(8)	C(5a)–N(2a)–Pb	121.2(7)
N(2b)–Pb–S(1a)	155.0(2)	N(2b)–Pb–S(1b)	58.6(2)	C(5a)–N(2a)–C(4a)	122(1)	C(4b)–N(2b)–Pb	118.0(7)
N(2b)–Pb–N(1c)	62.0(3)	N(2b)–Pb–N(2a)	125.5(3)	C(5b)–N(2b)–Pb	121.8(7)	C(5b)–N(2b)–C(4b)	120(1)
O(18)–Pb–S(1a)	72.8(2)	O(18)–Pb–S(1b)	72.6(2)	C(8b)–N(3c)–C(8a)	116(1)	C(4a)–C(3a)–N(1c)	118(1)
O(18)–Pb–N(1c)	70.3(3)	O(18)–Pb–N(2a)	84.9(3)	C(3a)–C(4a)–N(2a)	122(1)	C(6a)–C(5a)–N(2a)	118(1)
O(18)–Pb–N(2b)	83.0(3)	O(w)–Pb–S(1a)	113.7(2)	C(5a)–C(6a)–S(1a)	119.3(9)	C(8a)–C(7a)–S(1a)	109.0(8)
O(w)–Pb–S(1b)	132.6(2)	O(w)–Pb–N(1c)	73.1(3)	C(7a)–C(8a)–N(3c)	114(1)	C(4b)–C(3b)–N(1c)	117(1)
O(w)–Pb–N(2a)	69.8(3)	O(w)–Pb–N(2b)	89.1(3)	C(3b)–C(4b)–N(2b)	120(1)	C(6b)–C(5b)–N(2b)	118(1)
O(w)–Pb–O(18)	142.0(3)	C(6a)–S(1a)–Pb	97.0(4)	C(5b)–C(6b)–S(1b)	117.5(8)	C(8b)–C(7b)–S(1b)	109.9(8)
C(7a)–S(1a)–Pb	102.9(4)	C(7a)–S(1a)–C(6a)	101.1(6)	C(7b)–C(8b)–N(3c)	115(1)		
C(6b)–S(1b)–Pb	98.2(4)	C(7b)–S(1b)–Pb	104.2(4)				

Table 6 Selected bond lengths (Å) and angles (°) for complex **2**

Hg–S(1a)	3.090(3)	Hg–S(1b)	3.166(3)	N(2a)–C(5a)	1.418(13)	N(2b)–C(4b)	1.267(14)
Hg–N(1c)	2.554(9)	Hg–N(2a)	2.708(9)	N(2b)–C(5b)	1.429(13)	N(3c)–C(8a)	1.338(12)
Hg–N(2b)	2.738(8)	Hg–S(1d)	2.491(3)	N(3c)–C(8b)	1.369(13)	C(3a)–C(4a)	1.459(14)
Hg–S(1e)	2.437(3)	S(1a)–C(6a)	1.760(10)	C(5a)–C(6a)	1.412(14)	C(7a)–C(8a)	1.526(14)
S(1a)–C(7a)	1.809(12)	S(1b)–C(6b)	1.751(11)	C(3b)–C(4b)	1.492(16)	C(5b)–C(6b)	1.376(15)
S(1b)–C(7b)	1.815(13)	N(1c)–C(3a)	1.344(13)	C(7b)–C(8b)	1.492(14)	N(3c) ··· Hg	3.14
N(1c)–C(3b)	1.354(13)	N(2a)–C(4a)	1.304(13)				
S(1b)–Hg–S(1a)	114.8(1)	N(1c)–Hg–S(1a)	118.7(2)	C(7b)–S(1b)–C(6b)	100.6(6)	C(3a)–N(1c)–Hg	120.7(7)
N(1c)–Hg–S(1b)	118.5(2)	N(2a)–Hg–S(1a)	60.7(2)	C(3b)–N(1c)–Hg	120.5(7)	C(3b)–N(1c)–C(3a)	117.4(9)
N(2a)–Hg–S(1b)	173.4(2)	N(2a)–Hg–N(1c)	63.1(3)	C(4a)–N(2a)–Hg	114.7(7)	C(5a)–N(2a)–Hg	126.1(7)
N(2b)–Hg–S(1a)	171.8(2)	N(2b)–Hg–S(1b)	60.1(2)	C(5a)–N(2a)–C(4a)	119.0(9)	C(4b)–N(2b)–Hg	115.4(8)
N(2b)–Hg–N(1c)	62.8(3)	N(2b)–Hg–N(2a)	123.7(3)	C(5b)–N(2b)–Hg	125.4(7)	C(5b)–N(2b)–C(4b)	119(1)
S(1d)–Hg–S(1a)	69.4(1)	S(1d)–Hg–S(1b)	85.9(1)	C(8b)–N(3c)–C(8a)	117.4(9)	C(2b)–C(1c)–C(2a)	119(1)
S(1d)–Hg–N(1c)	86.4(2)	S(1d)–Hg–N(2a)	87.9(2)	C(3a)–C(2a)–C(1c)	119(1)	C(4a)–C(3a)–N(1c)	117.1(9)
S(1d)–Hg–N(2b)	103.1(2)	S(1e)–Hg–S(1a)	106.6(1)	C(4a)–C(3a)–C(2a)	120(1)	C(3a)–C(4a)–N(2a)	122(1)
S(1e)–Hg–S(1b)	95.5(1)	S(1e)–Hg–N(1c)	96.2(2)	C(6a)–C(5a)–N(2a)	118(1)	C(5a)–C(6a)–S(1a)	119.1(8)
S(1e)–Hg–N(2a)	90.5(2)	S(1e)–Hg–N(2b)	80.8(2)	C(8a)–C(7a)–S(1a)	108.2(7)	C(7a)–C(8a)–N(3c)	115.7(9)
S(1e)–Hg–S(1d)	176.0(1)	C(6a)–S(1a)–Hg	103.1(4)	C(4b)–C(3b)–N(1c)	117(1)	C(3b)–C(4b)–N(2b)	121(1)
C(7a)–S(1a)–Hg	106.3(4)	C(7a)–S(1a)–C(6a)	102.0(5)	C(6b)–C(5b)–N(2b)	118.1(9)	C(5b)–C(6b)–S(1b)	121.7(9)
C(6b)–S(1b)–Hg	101.2(4)	C(7b)–S(1b)–Hg	96.2(4)	C(8b)–C(7b)–S(1b)	109.8(8)	C(7b)–C(8b)–N(3c)	115(1)

comparative purposes. In this context, the Pb–S distances in this structure are close to the estimated sum of the Shannon ionic radius of eight-co-ordinate lead(II) (1.29 Å) and the van der Waals radius of sulfur (1.85 Å).[18] Of the Pb–O axial bonds, one is strong and the other relatively weak [Pb–O(18) 2.530(8) and Pb–O(w) 2.766(8) Å]. The non-linear O(w)–Pb–O(18) arrangement, with a bond angle of 142.0(3)°, may be attributed to the localisation of a stereochemically active $6s^2$ lone pair of electrons on the lead atom; significantly, replacement of Pb^{II} for Hg^{II}, see below, results in linear axial bonds to the central metal. Recent structural studies on the isoelectronic ion Bi^{III} have shown that a stereochemically active lone pair is promoted by the presence in the complex of covalent or partially covalent bonds.[19] The solution and structural data obtained in this work, together with the findings of other studies on Pb^{II},[20] are in keeping with this postulation.

The molecular structure of complex **2** is illustrated in Fig. 3, and bond lengths and angles in Table 6. In many respects the structure is similar to that of **1a**. The mercury atom is located asymmetrically within the macrocyclic cavity, being closer to the N_3 trimethine chelating fragment than the NS_2 chelating fragment. The metal geometry is again best described as a very distorted *nido*-hexagonal bipyramid in which the macrocycle occupies five of the 'equatorial' sites, once again leaving the pyridyl nitrogen of the sulfur end of the ligand unused [Hg ··· N(3c) 3.14 Å]; thiocyanate anions complete axial sulfur co-ordination to the mercury. In detail, there are a number of significant differences in the structure of **2** compared to that of **1a**. The axial bond angle S(1e)–Hg–S(1d) of 176.0(1)° is much more linear than the corresponding angle found in **1a**, and is almost perpendicular to the trimethine plane [S(1d)–Hg–N(1c) 86.4(2)°], as expected when there is no sterically active lone pair. The bond lengths between the mercury atoms and the sulfur atoms of the thiocyanate [Hg–S 2.491(3) and 2.437(3) Å] are much shorter than those to the sulfurs of the macrocycle [Hg–S 3.090(3) and 3.166(3) Å], indicating a stronger interaction for these than the former. The mercury atom is located 0.64 Å out of the mean plane of the trimethine nitrogens, giving the unusual appearance of bent co-ordinate bonds to these sp^2-hybridised nitrogens. (In this connection we note the weak mercury–proton coupling in the NMR spectrum). The asymmetric bonding of the mercury atom together with the aforementioned 'bent' interactions may indicate that the ion is too small for the cavity and that it is 'locked' into the complex by virtue of the

Table 7 Fractional atomic coordinates for complex **1a**

Atom	*x*	*y*	*z*
Pb	0.220 47(4)	0.163 19(4)	0.189 37(5)
S(1a)	0.458 6(2)	0.127 1(3)	0.281 8(3)
S(1b)	0.213 9(2)	0.384 8(3)	0.032 2(3)
C(1c)	0.119 8(7)	0.182 4(8)	0.369 8(8)
N(2a)	2.281 0(7)	0.038 7(9)	0.385 9(9)
N(2b)	0.052 2(7)	0.285 5(8)	0.156 4(8)
N(3c)	0.395 9(7)	0.232 7(9)	0.023 6(9)
C(1c)	0.007 2(11)	0.193 6(12)	0.563 8(12)
C(2a)	0.088 2(11)	0.125 0(12)	0.569 8(11)
C(3a)	0.144 2(9)	0.120 1(10)	0.471 5(11)
C(4a)	0.228 2(19)	0.045 5(11)	0.474 0(11)
C(5a)	0.353 1(10)	−0.043 2(11)	0.381 0(10)
C(6a)	0.438 5(9)	−0.014 1(10)	0.328 0(11)
C(7a)	0.502 8(10)	0.098 0(12)	0.135 6(12)
C(8a)	0.494 7(10)	0.204 9(11)	0.061 6(11)
C(9a)	0.581 5(10)	0.261 2(13)	0.026 2(13)
C(10c)	0.565 9(12)	0.348 0(12)	−0.051 1(15)
C(11a)	0.337 2(10)	−0.152 9(11)	0.421 0(12)
C(12a)	0.409 5(12)	−0.229 7(11)	0.411 0(12)
C(13a)	0.496 7(11)	−0.201 5(13)	0.360 5(12)
C(14a)	0.511 4(11)	−0.093 5(13)	0.317 5(12)
C(2b)	−0.019 0(10)	0.254 4(11)	0.460 2(12)
C(3b)	0.038 7(9)	0.243 4(10)	0.365 9(11)
C(4b)	0.005 5(9)	0.300 7(10)	0.249 2(11)
C(5b)	0.008 8(9)	0.322 3(9)	0.037 3(11)
C(6b)	0.079 3(9)	0.367 6(10)	−0.036 4(11)
C(7b)	0.273 7(9)	0.344 5(11)	−0.100 3(11)
C(8b)	0.384 8(10)	0.319 2(10)	−0.053 4(11)
C(9b)	0.467 4(10)	0.377 8(11)	−0.092 5(12)
C(11b)	−0.099 6(9)	0.310 8(11)	−0.011 9(12)
C(12b)	−0.136 5(10)	0.339 9(11)	−0.129 8(12)
C(13b)	−0.070 6(11)	0.383 2(12)	−0.202 9(12)
C(14b)	0.037 5(10)	0.398 2(10)	−0.157 0(11)
Cl(1)	0.200 5(2)	−0.004 6(3)	−0.116 7(3)
O(11)	0.257 6(7)	−0.039 3(8)	−0.001 2(8)
O(12)	0.273 1(8)	0.033 2(9)	−0.192 8(9)
O(13)	0.143 6(7)	0.091 1(8)	−0.088 1(8)
O(14)	0.129 6(10)	−0.092 9(9)	−0.185 6(12)
Cl(2)	0.249 2(3)	0.521 3(4)	0.595 3(3)
O(21)	0.192 4(13)	0.547 2(14)	0.682 6(14)
O(22)	0.249 5(15)	0.400 7(12)	0.574 5(14)
O(23)	0.228 1(11)	0.574 7(16)	0.486 8(12)
O(24)	0.353 3(13)	0.544 4(20)	0.644 1(17)
O(18)	0.302 6(7)	0.335 4(8)	0.341 1(8)
C(18)	0.390 6(12)	0.412 6(13)	0.330 3(14)
O(w)	0.086 2(7)	−0.036 6(8)	0.169 8(8)

Table 8 Fractional atomic coordinates for complex **2**

Atom	*x*	*y*	*z*
Hg	0.237 53(4)	0.199 07(5)	0.198 19(6)
S(1a)	0.454 4(2)	0.158 0(3)	0.250 6(4)
S(1b)	0.213 6(2)	0.406 2(3)	−0.000 7(4)
N(1c)	0.123 1(6)	0.149 7(8)	0.395 5(10)
N(2a)	0.277 3(7)	0.038 0(8)	0.384 2(10)
N(2b)	0.058 1(7)	0.267 2(7)	0.162 7(11)
N(3c)	0.381 8(6)	0.260 9(7)	−0.039 6(10)
C(1c)	0.027 1(10)	0.140 7(11)	0.642 1(15)
C(2a)	0.104 2(9)	0.083 0(10)	0.633 8(13)
C(3a)	0.149 5(8)	0.089 6(9)	0.509 1(12)
C(4a)	0.230 6(8)	0.030 8(9)	0.498 0(13)
C(5a)	0.348 2(8)	−0.030 2(9)	0.373 3(12)
C(6a)	0.434 7(8)	0.016 2(8)	0.306 1(12)
C(7a)	0.493 8(8)	0.147 6(9)	0.075 3(13)
C(8a)	0.478 0(8)	0.252 1(9)	−0.008 7(12)
C(9a)	0.559 4(8)	0.326 1(10)	−0.057 1(13)
C(10c)	0.538 8(10)	0.415 7(10)	−0.144 9(13)
C(11a)	0.332 4(8)	−0.141 6(10)	0.417 0(12)
C(12a)	0.403 0(10)	−0.205 3(10)	0.400 4(12)
C(13a)	0.489 4(10)	−0.157 5(11)	0.343 1(13)
C(14a)	0.506 4(8)	−0.048 8(10)	0.295 3(12)
C(2b)	−0.003 6(8)	0.200 3(10)	0.522 7(15)
C(3b)	0.046 3(8)	0.202 4(9)	0.403 9(13)
C(4b)	0.013 1(9)	0.262 2(10)	0.273 4(15)
C(5b)	0.016 3(8)	0.313 2(9)	0.034 7(13)
C(6b)	0.082 3(8)	0.375 5(9)	−0.050 9(14)
C(7b)	0.254 9(8)	0.352 2(11)	−0.157 4(14)
C(8b)	0.363 7(9)	0.347 7(10)	−0.125 9(12)
C(9b)	0.440 2(9)	0.424 1(10)	−0.181 4(14)
C(11b)	−0.087 8(9)	0.290 2(10)	−0.007 0(15)
C(12b)	−0.125 2(9)	0.333 5(12)	−0.132 8(17)
C(13b)	−0.060 7(11)	0.399 4(11)	−0.218 3(16)
C(14b)	0.040 9(10)	0.421 2(10)	−0.179 2(14)
S(1d)	0.347 9(2)	0.344 0(3)	0.370 7(4)
C(1d)	0.270 1(11)	0.418 2(13)	0.418 6(17)
N(1d)	0.219 5(9)	0.469 2(11)	0.463 8(15)
S(1e)	0.140 1(2)	0.052 7(3)	0.026 6(4)
C(1e)	0.225 4(9)	−0.003 0(10)	−0.036 9(13)
N(1e)	0.281 2(8)	−0.044 8(9)	−0.088 6(13)
O(18)	0.181 0(6)	0.650 5(7)	0.609 3(10)
C(18)	0.263 8(9)	0.681 9(11)	0.717 7(15)

strongly co-ordinated 'stopper' thiocyanates, leaving relatively weak interactions with the trimethine end of the ligand. Very few crystal structures of mercury(II) complexes of macrocyclic ligands are known. The present complex belongs to a small subgroup of structurally characterised mercury(II) complexes in which the mercury is bound *endo*-macrocyclically[21] as opposed to the alternative *exo*-macrocyclic mode of binding.[22]

As shown above, the N_4S_2 macrocycles L^1 and L^2 can be templated on the 'ions' Pb^{II}, Cd^{II}, Hg^{II} and Ag^{I}, and not with other ions of comparable radii such as Ca^{II} and Sr^{II}. This is in contrast to the template synthesis of the closely related N_6 macrocycles L^3 and L^4, which co-ordinate in a planar manner to the cavity-incorporated metal,[7] but is in accord with the template syntheses of the closely related N_4O_2 macrocycle in which ether groups correspond to the thioethers of L^1.[23] The origins of such a template discrimination could arise from a shape selectivity effect, the sp^3 heteroatoms of the macrocycle requiring a cup-shaped cavity for metal incorporation.

At a time when the utility of 18-membered, sexidentate crown ethers in the separation of Pb^{II} is being examined,[24] this work demonstrates the potential of the 18-membered N_4S_2 ligands as complexing agents for environmentally important heavy-metal ions. Although further investigations have been hampered by the apparent instability of the same ligands in the absence of the template ions (a thermodynamic template effect?), we are currently examining the interaction of the same metal ions with metal-free derivatives of the above macrocyclic complexes as well as the reduced acyclic precursor amine.

Acknowledgements

We thank the SERC for funding (to H. R. P. and S. W.).

References

1 G. W. Gokel, *Crown Ethers and Cryptands*, The Royal Society of Chemistry, Cambridge, 1991; L. F. Lindoy, in *Cation Binding by Macrocycles*, eds. Y. Inoue and G. W. Gokel, Marcel Dekker, New York, 1990, pp. 599–629; L. F. Lindoy, *The Chemistry of Macrocyclic Ligand Complexes*, Cambridge University Press, Cambridge, 1989,

pp. 185–191; *Synthesis of Macrocycles: The Design of Selective Agents* (*Progress in Macrocyclic Chemistry*), eds. R. M. Izatt and J. J. Christensen, Wiley, New York, 1987, vol. 3; *Host-Guest Complex Chemistry, Macrocycles*, eds. F. Vogtle and E. Weber, Springer, Berlin, Heidelberg, 1985; J. D. Lamb, R. M. Izatt, J. J. Christensen and D. J. Eatough, in *The Coordination Chemistry of Macrocyclic Compounds*, ed. G. A. Melson, Plenum, New York, 1979, pp. 145–217.

2 J. Hunter, B. P. Murphy and J. Nelson, *J. Chem. Educ.*, 1991, **68**, 59; K. R. Adam, S. Donnelly, A. J. Leong, L. F. Lindoy, B. J. McCool, A. Bashall, M. R. Dent, B. P. Murphy, M. McPartlin, D. E. Fenton and P. A. Tasker, *J. Chem. Soc., Dalton Trans.*, 1990, 1635; A. Bashall, M. McPartlin, B. P. Murphy, D. E. Fenton, S. J. Kitchen and P. A. Tasker, *J. Chem. Soc., Dalton Trans.*, 1990, 505; D. E. Fenton, B. P. Murphy, A. J. Leong, L. F. Lindoy, A. Bashall and M. McPartlin, *J. Chem. Soc., Dalton Trans.*, 1987, 2543; J. Nelson, B. P. Murphy, M. G. B. Drew, P. C. Yates and S. M. Nelson, *J. Chem. Soc., Dalton Trans.*, 1988, 1001; B. P. Murphy, J. Nelson, S. M. Nelson, M. G. B. Drew and P. C. Yates, *J. Chem. Soc., Dalton Trans.*, 1987, 123.

3 E. C. Constable, C. Sacht, G. Palo, D. A. Tocher and M. Truter, *J. Chem. Soc., Dalton Trans.*, 1993, 1307.

4 A. Bashall, M. McPartlin, B. P. Murphy, H. R. Powell and S. Waikar, 16th International Symposium on Macrocyclic Chemistry, Sheffield, August 1991.

5 D. E. Fenton, *Pure Appl. Chem.*, 1986, **58**, 1437; S. M. Nelson, *Pure Appl. Chem.*, 1980, **52**, 2461.

6 R. D. Rogers and A. H. Bond, *Inorg. Chim. Acta*, 1992, 192, 163 and refs. therein; A. Bashall, M. McPartlin, B. P. Murphy, D. E. Fenton, S. J. Kitchen and P. A. Tasker, *J. Chem. Soc., Dalton Trans.*, 1990, 505; K. R. Adam, S. Donnelly, A. J. Leong, L. F. Lindoy, B. J. McCool, A. Bashall, M. R. Dent, B. P. Murphy, M. McPartlin, D. E. Fenton and P. A. Tasker, *J. Chem. Soc., Dalton Trans.*, 1990, 1635; D. E. Fenton, B. P. Murphy, A. J. Leong, L. F. Lindoy, A. Bashall and M. McPartlin, *J. Chem. Soc., Dalton Trans.*, 1987, 2543; N. A. Bailey, D. E. Fenton, I. T. Jackson, R. Moody and C. Rodiguez de Barbarin, *J. Chem. Soc., Chem. Commun.*, 1983, 1463.

7 M. G. B. Drew, J. de O. Cabral, M. F. Cabral, F. S. Esho and S. M. Nelson, *J. Chem. Soc., Chem. Commun.*, 1979, 1033; J. de O. Cabral, M. F. Cabral, W. J. Cummins and M. G. B. Drew, *Inorg. Chim. Acta*, 1978, **30**, L313.

8 W. Baker, K. M. Buggle, J. F. W. McOmie and D. A. M. Watkin, *J. Chem. Soc.*, 1958, 3594.

9 D. Jerchel, J. Heider and H. Wagner, *Leibigs Ann. Chem.*, 1958, **613**, 153.

10 M. K. Cooper, P. J. Guerney and M. McPartlin, *J. Chem. Soc., Dalton Trans.*, 1982, 757.

11 G. M. Sheldrick, SHELX 76 program for crystal structure determination, University of Cambridge, 1976.

12 N. Walker and D. Stuart, *Acta Crystallogr., Sect. A*, 1983, **39**, 158.

13 *International Tables for X-Ray Crystallography*, Kynoch Press, Birmingham, 1974, vol. 4.

14 F. Teixidor, L. Escriche, J. Casabo, E. Molins and C. Miravitlles, *Inorg. Chem.*, 1986, **25**, 4060.

15 P. S. Marchetti, S. Bank, T. W. Bell, M. A. Kennedy and P. D. Ellis, *J. Am. Chem. Soc.*, 1989, **111**, 2063.

16 H.-J. Kuppers, K. Wieghardt, B. Nuber and J. Weiss, *Z. Anorg. Allg. Chem.*, 1989, **577**, 155; M. M. Olmstead, R. M. Kessler, H. Hope, M. D. Yanuck and W. K. Musker, *Acta Crystallogr., Sect. C*, 1987, **43**, 1890.

17 R. D. Shannon, *Acta Crystallogr., Sect. A*, 1976, **32**, 751.

18 L. Pauling, *The Nature of the Chemical Bond*, 3rd edn., Cornell University Press, Ithaca, 1960.

19 R. D. Rogers, A. H. Bond, S. Aguinaga and A. Reyes, *J. Am. Chem. Soc.*, 1992, **114**, 2967; R. D. Rogers, A. H. Bond and S. Aguinaga, *J. Am. Chem. Soc.*, 1992, **114**, 2960.

20 R. D. Rogers and A. H. Bond, *Inorg. Chim. Acta*, 1992, **192**, 163; R. D. Hancock, M. S. Shaikjee, S. M. Dobson and J. C. A. Boeyens, *Inorg. Chim. Acta*, 1988, **154**, 229.

21 M. G. B. Drew, S. G. McFall and S. M. Nelson, *J. Chem. Soc., Dalton Trans.*, 1979, 575; S. M. Nelson, S. G. McFall, M. G. B. Drew, A. bin Othman and N. B. Mason, *J. Chem. Soc., Chem. Commun.*, 1977, 167.

22 H. Adams, N. A. Bailey, D. E. Fenton, I. G. Ford, S. J. Kitchen, M. G. Williams, P. A. Tasker, A. J. Leong and L. F. Lindoy, *J. Chem. Soc., Dalton Trans.*, 1991, 1665; N. W. Alcock, N. Herron and P. Moore, *J. Chem. Soc., Dalton Trans.*, 1978, 394.

23 D. E. Fenton, B. P. Murphy, A. J. Leong, L. F. Lindoy, A. Bashall and M. McPartlin, *J. Chem. Soc., Dalton Trans.*, 1987, 2543.

24 E. P. Horwitz, M. L. Dietz and D. E. Fisher, *Anal. Chem.*, 1991, **63**, 522; D. B. Gomis and E. A. Garcia, *Analyst (London)*, 1990, **115**, 89.

Received 14*th January* 1994; *Paper* 4/00230J